Contribution of ion currents to beat-to-beat variability of action potential duration in canine ventricular myocytes

Norbert Szentandrássy[1,2], Kornél Kistamás[1], Bence Hegyi[1], Balázs Horváth[1], Ferenc Ruzsnavszky[1], Krisztina Váczi[1], János Magyar[1,3], Tamás Bányász[1], András Varró[4], Péter P. Nánási[1,2]

[1]Department of Physiology, Faculty of Medicine, University of Debrecen, Debrecen, Hungary

[2]Department of Dental Physiology and Pharmacology, Faculty of Dentistry, University of Debrecen, Debrecen, Hungary

[3]Division of Sport Physiology, Department of Physiology, Faculty of Medicine, University of Debrecen, Hungary

[4]Department of Pharmacology and Pharmacotherapy, University of Szeged, Szeged, Hungary

Running title: Beat-to-beat variability

Correspondence: Péter P. Nánási, M.D., Ph.D., D.Sc.
Department of Physiology, University of Debrecen,
H-4012 Debrecen, Nagyerdei krt 98, Hungary.
Phone/Fax: +36-52-255575 / +36-52-255116
E-mail: nanasi.peter@med.unideb.hu

Abstract Although beat-to-beat variability (short term variability, SV) of action potential duration (APD) is considered as a predictor of imminent cardiac arrhythmias, the underlying mechanisms are still not clear. In the present study, therefore, we aimed to determine the role of the major cardiac ion currents, APD, stimulation frequency and changes in the intracellular Ca^{2+} concentration ($[Ca^{2+}]_i$) on the magnitude of SV. Action potentials were recorded from isolated canine ventricular cardiomyocytes using conventional microelectrode techniques. SV was an exponential function of APD, when APD was modified by current injections. Drug-effects were characterized as *relative SV* changes by comparing the drug-induced changes in SV to those in APD according to the exponential function obtained with current pulses. *Relative SV* was increased by dofetilide, HMR 1556, nisoldipine and veratridine, while it was reduced by BAY K8644, tetrodotoxin, lidocaine, and isoproterenol. *Relative SV* was also increased by increasing the stimulation frequency and $[Ca^{2+}]_i$. In summary, relative SV is decreased by ion currents involved in the negative feedback regulation of APD (I_{Ca}, I_{Ks} and I_{Kr}), while it is increased by I_{Na} and I_{to}. We conclude that drug-induced effects on SV should be evaluated in relation with the concomitant changes in APD. Since *relative SV* was decreased by ion currents playing critical role in the negative feedback regulation of APD, blockade of these currents, or the beta-adrenergic pathway, may carry also some additional proarrhythmic risk in addition to their well-known antiarrhythmic action.

Keywords

short term variability – action potential duration – ion currents – canine myocytes – action potential configuration.

Introduction

Beat-to-beat variability of action potential duration (also called short term variability, SV) is an intrinsic property of various *in vivo* and *in vitro* mammalian cardiac preparations including the human heart [7, 8, 21]. In spite of the fact that SV is considered one of the best proarrhythmic predictors [1, 11, 22] (but see also Michael et al. 2007 [17]), its exact ionic mechanism is poorly understood. Involvement of many factors, such as stochastic gating of ion channels [14, 18], cell-to-cell coupling [27], action potential duration and morphology [6], stimulation frequency [12] and intracellular calcium handling [13] in modulation of SV have been reported, however, neither their relative contribution, nor the role of the specific cardiac ion currents have been identified in a well defined experimental model. Therefore, in absence of relevant human cellular electrophysiological data, canine ventricular myocytes were chosen to analyze experimentally the determinants of SV in the present study due to two reasons. (1) Canine ventricular myocytes are believed to resemble human ventricular cells regarding their action potential morphology and kinetics of the underlying ion currents [19, 20]; and (2) a large mass of *in vitro* and *in vivo* experimental data on beat-to-beat variability have been obtained in this species [1, 12, 13, 15, 22, 23].

Methods

Isolation of single canine ventricular myocytes

Adult mongrel dogs of either sex were anaesthetized with intramuscular injections of 10 mg/kg ketamine hydrochloride (Calypsol, Richter Gedeon, Hungary) + 1 mg/kg xylazine hydrochloride (Sedaxylan, Eurovet Animal Health BV, The Netherlands) according to protocols approved by the local ethical committee (license N^{o}: 18/2012/DEMÁB) in line with the ethical standards laid down in the 1964 Declaration of Helsinki and its later amendments. The hearts were quickly removed and placed in Tyrode solution. Single myocytes were obtained by enzymatic dispersion using the segment perfusion technique, as described previously [2, 3, 9, 16]. Briefly, a wedge-shaped section of the ventricular wall supplied by the left anterior descending coronary artery was dissected, cannulated

and perfused with oxygenized Tyrode solution. After removal of blood the perfusion was switched to a nominally Ca^{2+}-free Joklik solution (Minimum Essential Medium Eagle, Joklik Modification, Sigma) for 5 min. This was followed by 30 min perfusion with Joklik solution supplemented with 1 mg/ml collagenase (Type II. Worthington, Chemical Co.) and 0.2 % bovine serum albumin (Fraction V., Sigma) containing 50 μM Ca^{2+}. All other drugs were obtained from Sigma-Aldrich Co. (St. Louis, MO, USA). After gradually restoring the normal external Ca^{2+} concentration, the cells were stored in Minimum Essential Medium Eagle until use.

Recording of action potentials

All electrophysiological measurements were performed at 37 °C. The rod-shaped viable cells showing clear striation were sedimented in a plexiglass chamber of 1 ml volume allowing continuous superfusion (at a rate of 2 ml/min) with modified Krebs solution gassed with a mixture of 95 % O_2 and 5 % CO_2 at pH = 7.4. The modified Krebs solution contained (in mM): NaCl, 128.3; $NaHCO_3$, 21.4; KCl, 4.0; $CaCl_2$, 1.8; $MgCl_2$, 0.42; and glucose 10. Transmembrane potentials were recorded using 3 M KCl filled sharp glass microelectrodes having tip resistance between 20 and 40 MΩ. These electrodes were connected to the input of Multiclamp 700A, 700B or Axoclamp-2B amplifiers (Molecular Devices, Sunnyvale, CA, USA). The cells were paced through the recording electrode at steady cycle length of 1 s using 1-2 ms wide rectangular current pulses having amplitudes of twice the diastolic threshold. Since the cytosol was not dialyzed, time dependent changes in action potential morphology were negligible for the period of our experimental protocol lasting typically not longer than 25 min, as was demonstrated in **Fig. 1e**. Action potentials were digitized (at 200 kHz using Digidata 1322A, 1440A and 1200 A/D card, purchased from Axon Instruments Inc., Foster City, CA, USA) and stored for later analysis. Series of 50 consecutive action potentials were analyzed to estimate SV according to the following formula:

$$SV = \Sigma \left(\left| APD_{n+1} \textit{ minus } APD_n \right| \right) / [n_{beats} * \sqrt{2}]$$

where SV is short term variability, APD_n and APD_{n+1} indicate the durations of the n^{th} and $n+1^{th}$ APs, respectively, at 90% level of repolarization and n_{beats} denotes the number of

consecutive beats analyzed [12]. Changes in SV were typically presented as Poincaré plots where 50 consecutive APD values are plotted, each against the duration of the previous action potential.

Here is to be mentioned that all action potentials analyzed in the present study were normally driven ones, records taken in myocytes displaying early or delayed afterdepolarizations were excluded from evaluation.

Statistics

Results are expressed as mean ± SEM values. Statistical significance of differences was evaluated using one-way ANOVA followed by Student's t-test. Differences were considered significant when p was less than 0.05. Each given n value represents the number of cells / number of animals.

Results

Transmural distribution of SV

Since considerable differences are known to exist in the set and densities of ion currents, resulting in different action potential morphologies, in the various layers of the ventricular wall, SV was compared in myocytes dispersed from the subepicardial (EPI), subendocardial (ENDO) and midmyocardial (MID) regions of the left ventricle. SV was the greatest in the MID cells (2.93±0.07 ms) smallest in EPI cells (2.16±0.17 ms), and had an intermediate level in ENDO myocytes (2.53±0.16 ms) as demonstrated in **Fig. 1a-c**. Although all these transmural differences in APD and SV were statistically significant when analyzed using ANOVA ($p<0.05$), they were not related to the spike-and-dome configuration of action potentials observed in EPI or MID cells. When the transient outward K^+ current (I_{to}) was suppressed by 1 mM 4-aminopyridine in EPI cells, the spike-and-dome action potential morphology disappeared but SV decreased slightly (by 0.57±0.49 ms, N.S., n=9/6) instead of increasing. This concentration of 4-aminopyridine failed to modify APD significantly (not shown). As shown in **Fig. 1d**, the observed

transmural distribution of SV was largely proportional to APD values. Therefore, the relationship between SV and APD was further studied.

Relationship between SV and APD

To study the dependence of SV on APD, outward and inward current injections were applied in current clamp mode. The current pulses, having amplitudes varied from -600 to +70 pA, were injected throughout the full duration of the action potential except phase 0 (**Fig. 2a,b**). These experiments, similarly to all results discussed in the followings, were performed in midmyocardial cells. Using current pulses of various amplitudes allowed the modification of APD within a reasonably wide range (from 20 to 500 ms) in a way not related to exclusive interaction with one or another specific ion current. The results obtained by analyzing 117 data points (i.e. corresponding SV and APD values, each representing a group of 50 consecutive action potentials), are presented in **Fig. 2c-e**. As shown in **Fig. 2c** the SV-APD relationship follows exponential kinetics. Similarly, an exponential relationship was observed when the current-induced changes in SV and APD were analyzed (**Fig. 2d**). Furthermore, when the *relative* change in SV (defined as $\Delta SV / \Delta APD$) was plotted against the current-induced change in APD (ΔAPD), this relationship could also be fitted to an exponential function. From the ΔSV *versus* ΔAPD and $\Delta SV / \Delta APD$ *versus* ΔAPD relations one can estimate that a change in SV caused by any given drug or intervention is greater or less than the value predicted by the concomitant change in APD. The equations used for the fitting procedure together with their numerical solutions are presented in **Table 1**. The most important conclusion from these experiments is that any drug-induced change in SV must be evaluated in terms of *relative* SV, i.e. by comparing changes in SV to concomitant changes in APD.

Effect of the pacing cycle length

Since the duration of a cardiac action potential is strongly influenced by the frequency of stimulation, it was reasonable to study whether the frequency-dependent changes in SV are in line with the predictions of the APD changes. Both APD and SV increased with

lengthening of pacing cycle length (**Fig. 3a-d**). When each SV was plotted as a function of the corresponding APD value, and the exponential curve obtained from the experiments presented previously in **Fig. 2.** was superimposed, the experimental data gave a good fit to the curve – at least for cycle lengths longer than 0.5 s. SV values obtained at higher frequencies were larger than predicted by the APD-SV relationship indicating the possible contribution of factors other than APD at higher pacing frequencies (**Fig. 3e**).

Effect of changes in $[Ca^{2+}]_i$ on SV

There are various manipulations suitable for modulation of $[Ca^{2+}]_i$ experimentally - the majority of them involves interactions with sarcoplasmic reticular Ca^{2+} handling. Instead of these, the simplest strategy was followed in the present study - based on the assumption that if the cell is loaded directly with Ca^{2+}, it must increase $[Ca^{2+}]_i$, and conversely, $[Ca^{2+}]_i$ must be reduced by an intracellularly applied Ca^{2+}-chelator. Exposure the cells to the Ca^{2+}-ionophore A 23187 (1 μM for 25 min) significantly shortened, while loading the cells with the cell-permeant acetoxy-methylesther form of the Ca^{2+} chelator BAPTA (using 5 μM BAPTA-AM for 25 min) strongly lengthened APD, although SV was not modified significantly by these interventions (**Fig. 4a-d**). However, as demonstrated in **Fig. 4e**, A 23187 increased, while BAPTA-AM decreased the *relative* SV when it was expressed as a function of APD change, i.e. as a $\Delta SV / \Delta APD$ ratio.

Contribution of the major ion currents to modulation of beat-to-beat variability: role of K^+ currents

The role of the various ion currents in modulation of SV can be best studied by using their selective activators and inhibitors. Contribution of five K^+ currents, the rapid delayed rectifier (I_{Kr}), the slow delayed rectifier (I_{Ks}), the transient outward current (I_{to}) and the inward rectifier (I_{K1}) was studied using their specific blockers: dofetilide, HMR 1556, chromanol 293B in the presence of HMR 1556, and $BaCl_2$, respectively. The ATP-sensitive K^+ current ($I_{K\text{-}ATP}$) was activated by lemakalim (**Fig. 5a-e**). Plotting the results

in the way as it was done in **Fig. 2c-e** revealed the specific effects of these agents on SV both absolutely and relatively (**Fig. 5f-h**). Accordingly, the I_{Kr} inhibitor dofetilide (10, 30, 100 and 300 nM) increased both APD and SV, however, its effect on SV was significantly stronger than its effect on APD (relative enhancement of SV). Similar effect could be observed with the selective I_{Ks} blocker HMR 1556 (0.5 µM), which agent caused only a small, but statistically significant lengthening of APD combined with a pronounced increase in SV. This can be best visualized in **Fig. 5h**, where the ΔSV / ΔAPD values were displayed *versus* ΔAPD. The diamond representing HMR 1556 is located far above the curve in the positive ΔAPD range. This indicates that the SV-increasing effect of HMR 1556 is much greater than predicted by the earlier discussed APD-SV relationship - in spite of the fact that I_{Ks} is considered to be a weak current in canine ventricular myocytes under baseline conditions [24, 26]. A relatively selective I_{to}-blockade can be achieved by applying chromanol 293B in the presence of HMR 1556 [25]. Exposure of myocytes to 100 µM chromanol 293B revealed that suppression of I_{to} decreased SV without significant alterations in APD, a result similar to previously obtained with 1 mM 4-aminopyridine. That is why the downward triangle, indicating chromanol 293B, is located also far above the curve (**Fig. 5h**). Increasing concentrations of lemakalim (0.1, 0.3, 1 and 5 µM) were used to shorten APD. Lemakalim decreased both SV and APD, but data points remained on the curve indicating that this current has little specific influence on SV. Suppression of I_{K1} with $BaCl_2$ (gradually increasing $BaCl_2$ concentration from 0.3 to 5 µM) increased APD and SV, but in this case the SV-increasing effect was weaker than predicted by the APD-SV relationship, suggesting that *relative* SV might be increased by I_{K1}. However, as it is clearly seen in **Fig. 5d**, $BaCl_2$ caused strong triangulation of action potentials, defined as a difference between the APD_{90} and APD_{50} values. Triangulation was 47±3 ms under control conditions, which increased to 90±11 ms in the presence of 5 µM $BaCl_2$ ($p<0.05$). Assuming that APD measured close to the plateau level may be more relevant to control action potential repolarization than APD_{90} itself, data points obtained with 5 µM $BaCl_2$ should be shifted leftwards on the horizontal axis in **Fig. 5f-h** by 43 ms for the sake of better comparability. Considering these corrections due to triangulation, each $BaCl_2$ data point touched the

exponential curve (not shown) indicating that I_{K1} is a current largely indifferent regarding the modulation of SV.

Contribution of inward currents

The role of Na^+ current (I_{Na}) was examined by suppression of I_{Na} using TTX and lidocaine, or alternatively, by activation of the current by veratridine (**Fig. 6a-c**). As expected, veratridine (10, 30 and 100 nM) increased both APD and SV in a concentration-dependent manner, while both parameters were simultaneously decreased by tetrodotoxin (TTX, 3 µM) and lidocaine (50 µM). Importantly, the SV-decreasing effect of I_{Na} inhibition, as well as the enhancement of SV caused by veratridine, were larger than predicted by the APD-SV relationship (**Fig. 6f-h**), congruently with an SV increasing action of I_{Na}. The other inward current under investigation was the L-type Ca^{2+} current (I_{Ca}). It was blocked by 1 µM nisoldipine and enhanced by 20 nM or 200 nM of BAY K8644 (**Fig. 6d,e**). Nisoldipine increased SV (by 0.52±0.19 ms) while APD was strongly shortened (by 103±7 ms), both effects were statistically significant ($p<0.05$, n=19/13). BAY K8644 increased APD significantly in 20 nM as well as 200 nM concentrations (APD-lengthening of 38±4 and 82±8 ms were observed in 12/6 and 21/9 myocytes, respectively, $p<0.05$). SV was not altered by 20 nM BAY K8644, but it was increased by 1.96±0.26 ms in the presence of 200 nM BAY K8644. As demonstrated in **Fig. 6f-h**, these changes in SV corresponded to a *relative* reduction of SV when compared to the concomitant lengthening of APD. In other words, SV was strongly diminished by I_{Ca}.

Offsetting the effects of APD changes

The best approach to separate the contribution of a specific ion current to modulating SV from the effect of the concomitant APD-change is to apply an electrical or pharmacological compensation. The former strategy was used in the experiments presented in **Fig. 7a-f**, where the APD-lengthening effects of 0.1 µM dofetilide, 5 µM $BaCl_2$, 0.1 µM veratridine and 0.2 µM BAY K8644 were offset using outward current

pulses with constant, properly chosen amplitude. Similarly, the APD-shortening effects of 3 μM tetrodotoxin and 1 μM nisoldipine were compensated using inward current pulses (**Fig. 7e,f**). After full compensation for the dofetilide-induced lengthening of APD a significant elevation of SV persisted (**Fig. 7a**), while in the case of $BaCl_2$ the enhancement of SV was eliminated by restoring the original value of APD. More specifically, SV, measured after compensation for the barium-induced lengthening of APD, fell below the control level of SV (**Fig. 7b**). However, applying the argumentation used in the case of **Fig. 5d**, based on the barium-induced triangulation of action potentials, APD_{50} was overcompensated by the applied outward current. This is in line with our previously discussed finding, i.e. suggesting that I_{K1} is really an indifferent current regarding its possible influence on SV. Similarly to results obtained with dofetilide, SV remained elevated in the presence of veratridine even if APD was fully compensated for (**Fig. 7c**) – in contrast to BAY K8644, which resulted in a subnormal level of SV after compensation for the APD-changes (**Fig. 7d**). When I_{Na} was blocked by tetrodotoxin, the SV values were lower than control following compensation of APD (**Fig. 7e**), while in the presence of the I_{Ca} blocker nisoldipine the drug-induced elevation of SV was further increased by the inward current pulse applied for offsetting the APD-changes (**Fig. 7f**).

Since one may argue that electrical compensation of APD-changes may shift the membrane potential to one or another direction, pharmacological compensation was also used in some experiments (**Fig. 7g-j**). In this case the APD-lengthening effects of dofetilide and veratridine were compensated by lemakalim (using properly chosen concentrations in each experiment), while the APD-shortening effects of tetrodotoxin and nisoldipine were compensated by $BaCl_2$. Although these compensations resulted in full restoration of the initial APD_{90} values, SV remained elevated in the presence of dofetilide and veratridine, became higher than control in nisoldipine and lower than control in tetrodotoxin. In summary, electrical and pharmacological compensation strategies yielded largely identical results corroborating the specific SV-lowering effects of I_{Kr} and I_{Ca}, as well as the SV-increasing effects of I_{Na}. It must be emphasized, however, that the most dramatic effect was observed with nisoldipine, independently of the way of compensation, highlighting the pivotal role of I_{Ca} in controlling SV.

Effect of isoproterenol

Summarizing the results above it could be concluded that two currents, namely I_{Ca} and I_{Ks}, were very effective in reducing the *relative* SV. If this is true, isoproterenol (ISO) is expected to decrease SV markedly, since this drug is known to increase both I_{Ca} and I_{Ks} simultaneously. ISO (10 nM) caused a small, although statistically significant shortening in APD at 1 Hz (reduction of 25±3 ms, $p<0.05$, n=13/5), which was accompanied with a robust decrease in SV (reduction of 0.89±0.09 ms, $p<0.05$, n=13/5), which was much larger than predicted by the APD-SV relationship (**Fig. 8a-c**). Indeed, the lowest SV could be observed at close to normal APD values in the presence of 10 nM ISO. Since ISO is known to increase $[Ca^{2+}]_i$, and changes in $[Ca^{2+}]_i$ were shown to influence *relative* SV, the effects of ISO were studied also after the exposure to 5 μM BAPTA-AM for 25 min. As seen previously, pretreatment with BAPTA-AM lengthened APD markedly without significantly affecting SV. In the presence of BAPTA-AM SV was decreased and APD was shortened by ISO similarly to results observed without BAPTA-AM (**Fig. 8d-e**). The effect of ISO on *relative SV* was largely similar in the presence and absence of BAPTA-AM, indicating that the effect of ISO on SV was not related to the concomitant changes in $[Ca^{2+}]_i$, it was rather caused by the ISO-induced augmentation of I_{Ca} and I_{Ks}. Supporting this conclusion, $\Delta SV / \Delta APD$ values were identical in the absence and presence of BAPTA-AM (0.043±0.007 (n=13/5) and 0.045±0.009 (n=7/4), respectively, N.S.).

The effect of 10 nM ISO was studied also at various pacing cycle lengths. In these experiments SV was determined by analyzing 10 consecutive action potentials only in order to limit the duration of the measurement. Although both the ISO-induced shortening of APD and reduction of SV increased with increasing the cycle length of stimulation (**Fig. 8f-g**), the *relative SV* - as demonstrated in **Fig. 8h** - progressively decreased at longer cycle lengths.

Discussion

The main goal of the present study was to separate SV changes related to inhibition of a specific ion current from those attributable to concomitant changes in APD. This approach allows for separation of ion currents to APD-stabilizing, therefore potentially antiarrhythmic currents (ones *decrease relative SV*) and to those which *increase relative SV*. Members of this latter group cause instability of APD, therefore they can be considered potentially arrhythmogenic. Using these categories based on predictions of arrhythmia incidence, 3 currents could be identified as APD-stabilizer: I_{Ca}, I_{Ks} and I_{Kr}. I_{Na} and I_{to} were found to increase instability of APD, while I_{K1} and $I_{K\text{-}ATP}$ appeared to be indifferent. These results provide an essentially new interpretation of beat-to-beat variability suggesting that the well-known negative feed-back regulation of APD may be an important factor of SV-modulation.

Effects of several ion channel modifiers (including dofetilide [12], HMR 1556 [12], ATX-II [12] and isoproterenol [13] in canine, while tetrodotoxin [27] and intracellular EGTA [27] in guinea pig ventricular cells) on the magnitude of beat-to-beat variability have been extensively studied, however, the changes in SV were not correlated by the investigators with the concomitant APD changes. The first approach to make such a distinction was the recent study of Heijman et al. [6], although it was an *in silico* analysis. Present results, however, have confirmed many of their predictions: I_{Na} and I_{Kr} have great impact on SV, I_{Kr} is an APD-stabilizing, while I_{Na} and I_{to} are APD-unstabilizing currents. I_{Ks} was estimated also as an APD-stabilizing current (having larger impact on SV than on APD) - in line with our observations, but only our analysis, based on comparison of ΔSV / ΔAPD changes, was able to highlight the importance of this interaction in the case of I_{Ks}. The largest difference between our and their results was found in the role of I_{Ca}. Although I_{Ca} was considered to be APD-stabilizing by both studies, it was the most important modulator in our experiments, as indicated by the results obtained with nisoldipine and BAY K8644 - in contrast to the moderate effect on SV proposed by the simulation in Fig. 3 of the study of Heijman et al. [6].

According to the conventional interpretation of beat-to-beat variability, it is due to the stochastic behavior of ion channel gating [14, 18]. Without questioning the contribution of this mechanism, here we propose another (probably more relevant) one to explain the observed changes in SV. Physiological control of APD is based on the

following well-known negative feed-back regulation scheme: prolongation of APD (e.g. due to the enhancement of an inward current) results in elevation of the plateau, which in turn accelerates the activation of I_{Kr} and I_{Ks} leading finally to a shortening of APD. Accordingly, those currents which are known to be critical members of this feed-back loop - namely I_{Ca}, I_{Kr} and I_{Ks} - are expected to decrease the variability of APD, and their inhibition may have an opposite effect. This interpretation provides some explanation for the following question: why I_{Ca} decreases while late I_{Na} increases APD. This is not evident since both currents are inwardly directed, tending to increase APD together with its variability. The crucial difference between I_{Ca} and late I_{Na} is that the former is active mainly during the initial part of the plateau [2], while the latter is dominant during the late plateau [10, 28]. As a consequence, I_{Ca} has a chance to shift the *early* plateau upwards allowing for faster and stronger activation of I_{Kr} and I_{Ks}, while in the case of late I_{Na} these changes develop later in time and in a less pronounced way. In line with this, the SV-increasing effect of late I_{Na} is strong because its activation overlaps the late plateau, where the membrane resistance is the highest [27], consequently, a relatively small inward shift in the net membrane current may result in a large prolongation of APD [3, 4]. This gives also the physical basis of the exponential relationship between SV and APD, as was predicted by the simulations of Heijman et al. [6] and confirmed experimentally by the present work.

In addition to action potential duration, the morphology of action potential was also suggested to be an important determinant of SV [6]. Heijman et al. simulated square-like action potential configuration by decreasing both I_{Ca} and I_{to}, while triangulation was achieved by strongly reducing I_{K1}. SV was dramatically elevated when it was simulated for a square-like action potential, on the contrary, triangulation decreased *relative* SV. Indeed, characteristic changes in action potential morphology can be attributed to modifications of many cardiac ion currents, e.g. suppression of I_{Ca} by nisoldipine results in plateau depression and square-like morphology. Similarly, suppression of I_{K1} caused triangulation of action potentials, i.e. smaller increase of APD_{50} than that of APD_{90}. Since the plateau level is critical in the negative feed-back regulation of APD, its duration is overestimated by APD_{90} in case of triangulation. This is why I_{K1} can not be considered as a potentially proarrhythmic current in dogs in spite of the reduction of *relative SV*

observed in $BaCl_2$. Although modification of SV observed in these examples is likely mediated by a change in action potential morphology, this is not always the case. For example, exposure of EPI myocytes to 4-aminopyridine converted action potential morphology from EPI to ENDO, but SV was not increased accordingly. Furthermore, SV was reduced by ISO very effectively without causing triangulation.

Our results regarding the effects of the stimulation cycle length on SV is similar to those of Johnson et al. [12], both studies showing an elevation of SV with increasing the cycle length. It might be tempting to associate these frequency-dependent changes in SV with the corresponding changes in the amplitude of specific ion currents. Since I_{Ca} is known to increase, while I_{Ks} is to decrease with increasing the cycle length of stimulation, the value of this approach seems to be limited. However, we have shown also that at cycle lengths of 700 ms or longer the changes in SV was likely due to the concomitant alterations of APD, since no change in *relative SV* could be observed within this frequency range. Specific cycle length-dependent changes in SV could be observed only at the shortest cycle lengths, where $[Ca^{2+}]_i$ could probably be elevated. Indeed, manipulation of $[Ca^{2+}]_i$ resulted in the expected change in the relative SV, which increased and decreased together with the changes in $[Ca^{2+}]_i$. In line with this assumption, the ISO-induced reduction of *relative SV* also increased with increasing the cycle length of stimulation. Accordingly, the ISO-induced reduction of SV was not significant at the shortest cycle length of 0.3 s, while it became progressively dominant at longer cycle lengths (including the range between 0.5 and 1 s, corresponding to the physiological heart rate in humans). It can be speculated that the ISO-induced reduction of relative SV could partially be offset by the elevated $[Ca^{2+}]_i$ at faster driving rates. It is worth mentioning that alternans was not observed even at the shortest cycle length of 300 ms - in contrast to the results of Johnson et al. [12]. This was likely the consequence of the bicarbonate content of our Krebs solution, which is known to provide an excellent intracellular buffering, decreasing thus the probability of alternans [5]. We have intentionally chosen the simplest way to manipulate $[Ca^{2+}]_i$, since both chelation of $[Ca^{2+}]_i$ and increasing the calcium entry using a calcium ionophore are expected to yield steady changes in $[Ca^{2+}]_i$, relatively independent of the cardiac cycle. This allowed a qualitative prediction of SV changes associated with variation of $[Ca^{2+}]_i$, but is obviously not suitable for modeling

the consequences of dynamic $[Ca^{2+}]_i$ changes occurring when transports between the sarcoplasmic reticulum and the cytosol are active.

In this investigation the possible contribution of one or another ion current to SV was studied by using specific activators and inhibitors of the ion channel in question. We tried to apply these agents in relatively selective concentrations (i.e. at concentrations resulting dominantly action on the targeted ion channel), while in some cases a series of concentrations have been applied. Serious problem with drug-selectivity arose only in the case of 4-aminopyridine, which is not selective blocker of I_{to} - not even at the concentration of 1 mM. Therefore selective suppression of I_{to} could be only achieved by using 100 μM chromanol 293B (of course in the presence of HMR 1556, since chromanol 293B is also known to inhibit I_{Ks}). Regarding the Ca^{2+} ionophore A 23187 and the Ca^{2+} chelator BAPTA-AM, the applied concentrations (1 and 5 μM, respectively) were chosen by convention, since the amount of calcium entry or calcium chelation depends primarily on the time of exposure.

In addition to the better understanding of the mechanism of beat-to-beat variability, there is one - quite annoying - practical implication of the present work. We have shown that I_{Kr}, I_{Ks} and I_{Ca} act to reduce short term variability. These are the currents being generally suppressed by class 3 and 4 antiarrhythmics, respectively. Furthermore, 10 nM ISO was the most effective agent to diminish relative SV out of all drugs tested. Class 2 antiarrhythmics, which are beta-receptor blockers, are expected to suppress this apparently beneficial adrenergic activity. Although we do not intend to suggest that adrenergic activation itself would be antiarrhythmic, it must be clearly seen that it has antiarrhythmic properties as well. Putting together, almost all of the presently applied antiarrhythmic agents (including the less side-effect carrying beta-blockers) may potentially increase the beat-to-beat variability of action potential duration limiting this way their antiarrhythmic potencies.

Acknowledgements

Financial support was provided by grants from the Hungarian Scientific Research Fund (OTKA-K100151, OTKA-K109736, OTKA-K101196, OTKA-PD101171 and OTKA-

NK104331). Further support was obtained from the Hungarian Government and the European Community (TAMOP-4.2.2.A-11/1/KONV-2012-0045 and TAMOP-4.2.2/B-10/1-2010-0024 research projects). Research of KK and HB was supported by the European Union and the State of Hungary, co-financed by the European Social Fund in the framework of TÁMOP-4.2.4.A/2-11/1-2012-0001 'National Excellence Program'. The authors thank Miss Éva Sági for her excellent technical assistance. The authors declare that they have no conflict of interest.

References

1. Abi-Gerges N, Valentin JP, Pollard CE (2010) Dog left ventricular midmyocardial myocytes for assessment of drug-induced delayed repolarization: short-term variability and proarrhythmic potential. Br J Pharmacol 159:77-92. doi: 10.1016/S0008-6363(02)00853-2
2. Bányász T, Fülöp L, Magyar J, Szentandrássy N, Varró A, Nánási PP (2003) Endocardial versus epicardial differences in L-type calcium current in canine ventricular myocytes studied by action potential voltage clamp. Cardiovasc Res 58:66-75. doi: 10.1016 / S0008-6363(02)00853-2
3. Bányász T, Horváth B, Virág L, Bárándi L, Szentandrássy N, Harmati G, Magyar J, Marangoni S, Zaza A, Varró A, Nánási PP (2009) Reverse rate dependency is an intrinsic property of canine cardiac preparations. Cardiovasc Res 84:237-244. doi: 10.1093/cvr/cvp213
4. Bárándi L, Virág L, Jost N, Horváth Z, Koncz I, Papp R, Harmati G, Horváth B, Szentandrássy N, Bányász T, Magyar J, Zaza A, Varró A, Nánási PP (2010) Reverse rate-dependent changes are determined by baseline action potential duration in mammalian and human ventricular preparations. Basic Res Cardiol 105:315-323. doi: 10.1007/s00395-009-0082-7
5. Fülöp L, Szigeti G, Magyar J, Szentandrássy N, Ivanics T, Miklós Z, Ligeti L, Kovács A, Szénási G, Csernoch L, Nánási PP, Bányász T (2003) Differences in electrophysiological and contractile properties of mammalian cardiac tissues in bicarbonate- and HEPES-buffered solutions. Acta Physiol Scand 178:11-18. doi: 10.1046/j.1365-201X.2003.01114.x
6. Heijman J, Zaza A, Johnson DM, Rudy Y, Peeters RLM, Volders PGA, Westra RL (2013) Determinants of beat-to-beat variability of repolarization duration in the canine ventricular myocyte: a computational analysis. PLOS Comput Biol 9: e1003202. doi: 10.1371/journal.pcbi.1003202
7. Hinterseer M, Beckmann BM, Thomsen MB, Pfeufer A, Dalla Pozza R, Loeff M, Netz H, Steinbeck G, Vos MA, Kääb S (2009) Relation of increased short-term

variability of QT interval to congenital long-QT syndrome. Am J Cardiol 103:1244-1248. doi: 10.1016/j.amjcard.2009.01.011

8. Hinterseer M, Beckmann BM, Thomsen MB, Pfeufer A, Ulbrich M, Sinner MF, Perz S, Wichmann HE, Lengyel C, Schimpf R, Maier SK, Varró A, Vos MA, Steinbeck G, Kääb S (2010) Usefulness of short-term variability of QT intervals as a predictor for electrical remodeling and proarrhythmia in patients with nonischemic heart failure. Am J Cardiol 106:216-220. doi: 10.1016/j.amjcard.2010.02.033.
9. Horváth B, Magyar J, Szentandrássy N, Birinyi P, Nánási PP, Bányász T (2006) Contribution of I_{Ks} to ventricular repolarization in canine myocytes. Pflügers Arch 452:698-706. doi: 10.1007/s00424-006-0077-2
10. Horvath B, Banyasz T, Jian Z, Hegyi B, Kistamas K, Nanasi PP, Izu LT, Chen-Izu Y (2013) Dynamics of the late Na^+ current during cardiac action potential and its contribution to afterdepolarizations. J Mol Cell Cardiol 64:59-68. doi: 10.1016/j.yjmcc.2013.08.010
11. Jacobson I, Carlsson L, Duker G (2011) Beat-by-beat QT interval variability, but not QT prolongation per se, predicts drug-induced torsades de pointes in the anaesthetised methoxamine-sensitized rabbit. J Pharmacol Toxicol Methods 63:40-46. doi: 10.1016/j.vascn.2010.04.010
12. Johnson DM, Heijman J, Pollard CE, Valentin JP, Crijns HJ, Abi-Gerges N, Volders PG (2010) I_{Ks} restricts excessive beat-to-beat variability of repolarization during beta-adrenergic receptor stimulation. J Mol Cell Cardiol 48:122-130. doi: 10.1016/j.yjmcc.2009.08.033
13. Johnson DM, Heijman J, Bode EF, Greensmith DJ, Van der Linde H, Abi-Gerges N, Eisner DA, Trafford AW, Volders PG (2013) Diastolic spontaneous calcium release from the sarcoplasmic reticulum increases beat-to-beat variability of repolarization in canine ventricular myocytes after β-adrenergic stimulation. Circ Res 112:246-256. doi: 10.1161/CIRCRESAHA.112.275735
14. Lemay M, de Lange E, Kucera JP (2011) Effects of stochastic channel gating and distribution on the cardiac action potential. J Theor Biol 281:84-96. doi: 10.1016/j.jtbi.2011.04.019

15. Lengyel C, Varró A, Tábori K, Papp JG, Baczkó I (2007) Combined pharmacological block of I_{Kr} and I_{Ks} increases short-term QT interval variability and provokes torsades de pointes. Br J Pharmacol 151:941-951. doi: 10.1038/sj.bjp.0707297
16. Magyar J, Iost N, Körtvély Á, Bányász T, Virág L, Szigligeti P, Varró A, Papp JGy, Nánási PP (2000) Effects of endothelin-1 on calcium and potassium currents in undiseased human ventricular myocytes. Pflügers Arch 441:144-149. doi: 10.1007/s004240000400
17. Michael G, Dempster J, Kane KA, Coker SJ (2007) Potentiation of E-4031-induced torsade de pointes by HMR1556 or ATX-II is not predicted by action potential short-term variability or triangulation. Br J Pharmacol 152:1215-1227. doi: 10.1016 / S0008-6363(02)00853-2
18. Pueyo E, Corrias A, Virág L, Jost N, Szél T, Varró A, Szentandrássy N, Nánási PP, Burrage K, Rodríguez B (2011) A multiscale investigation of repolarization variability and its role in cardiac arrhythmogenesis. Biophys J 101:2892-2902. doi: 10.1016/j.bpj.2011.09.060
19. Szabó G, Szentandrássy N, Bíró T, Tóth BI, Czifra G, Magyar J, Bányász T, Varró A, Kovács L, Nánási PP (2005) Asymmetrical distribution of ion channels in canine and human left ventricular wall: epicardium versus midmyocardium. Pflugers Arch 450:307-316. doi:10.1007/s00424-005-1445-z
20. Szentadrássy N, Bányász T, Bíró T, Szabó G, Tóth BI, Magyar J, Lázár J, Varró A, Kovács L, Nánási PP (2005) Apico-basal inhomogeneity in distribution of ion channels in canine and human ventricular myocardium. Cardiovasc Res 65:851-860. doi:10.1016/j.cardiores.2004.11.022
21. Tereshchenko LG, Han L, Cheng A, Marine JE, Spragg DD, Sinha S, Dalal D, Calkins H, Tomaselli GF, Berger RD (2010) Beat-to-beat three-dimensional ECG variability predicts ventricular arrhythmia in ICD recipients. Heart Rhythm 7:1606-1613. doi: 10.1016/j.hrthm.2010.08.022
22. Thomsen MB, Verduyn SC, Stengl M, Beekman JD, de Pater G, van Opstal J, Volders PG, Vos MA (2004) Increased short-term variability of repolarization

predicts d-sotalol-induced torsades de pointes in dogs. Circulation 110:2453-2459. doi: 10.1161/01.CIR.0000145162.64183.C8

23. Van der Linde H, Van de Water A, Loots W, Van Deuren B, Lu HR, Van Ammel K, Peeters M, Gallacher DJ (2005) A new method to calculate the beat-to-beat instability of QT duration in drug-induced long QT in anesthetized dogs. J Pharmacol Toxicol Methods 52:168-177. doi: 10.1016/j.vascn.2005.03.005
24. Varro A, Balati B, Iost N, Takacs J, Virag L, Lathrop DA, Lengyel Cs, Tálosi L, Papp JG (2000) The role of the delayed rectifier component I_{Ks} in dog ventricular muscle and Purkinje fibre repolarization. J Physiol 523:67-81. doi:10.1111/j.1469-7793.2000.00067.x
25. Virág L, Jost N, Papp R, Koncz I, Kristóf A, Kohajda Zs, Harmati G, Carbonell-Pascual B, Ferrero JM Jr, Papp JG, Nánási PP, Varró A (2011) Analysis of the contribution of I_{to} to repolarization in canine ventricular myocardium. Br J Pharmacol 164:93-105. doi: 10.1111/j.1476-5381.2011.01331.x.
26. Volders PG, Stengl M, van Opstal JM, Gerlach U, Spatjens RL, Beekman JD, Sipido KR, Vos MA (2003) Probing the contribution of I_{Ks} to canine ventricular repolarization: Key role for β-adrenergic receptor stimulation. Circulation 107:2753-2760. doi:10.1161/01.CIR.0000068344.54010.B3
27. Zaniboni M, Pollard AE, Yang L, Spitzer KW (2000) Beat-to-beat repolarization variability in ventricular myocytes and its suppression by electrical coupling. Am J Physiol Heart Circ Physiol 278:H677-H687. ISSN: 0363-6135
28. Zaza A, Rocchetti M (2013) The late Na^+ current – origin and pathophysiological relevance. Cardiovasc Drugs Ther 27:61-68. doi: 10.1007/s10557-012-6430-0

Table 1. Monoexponential fitting of the SV – APD relationship obtained by varying the amplitude of the injected current

Eq.	**y_0**	**A**	**T**	**r^2**
(1)	0 ms	0.56 ms	131 ms	0.98
(2)	-2.39 ms	2.37 ms	97 ms	0.97
(3)	0.008	0.016	129	0.82

Eq. (1) $SV = SV_0 + A * e^{APD / T}$
$y_0 = SV_0 = 0$

Eq. (2) $\Delta SV = \Delta SV_0 + A * e^{\Delta APD / T}$
$y_0 = \Delta SV_0$

Eq. (3) $\Delta SV / \Delta APD = (\Delta SV/\Delta APD)_0 + A * e^{(\Delta SV/\Delta APD) / T}$
$y_0 = (\Delta SV/\Delta APD)_0$

Data were obtained using inward and outward current injections (having amplitudes of -600, -500, -400, -300, -200, -80, -40, 0, +30, +40, +50, +60 and +70 pA) during the full duration of the action potential except phase 0. 117 individual data points, obtained from 9 myocytes of 8 dogs, were fitted to an exponential function described by Eq. (1), Eq. (2) or (Eq. 3), as pertinent. APD: action potential duration, SV: short term variability, r^2: regression coefficient, y_0 = minimum value of ordinate.

Figure legends

Fig. 1 Transmural distribution of beat-to-beat variability (SV) in canine ventricular myocardium. Tissue chunks originating from subepicardial (EPI), subendocardial (ENDO) and midmyocardial (MID) layers were isolated separately, then SV and APD were determined for each cell. **a**: Superimposed sets containing 50 consecutive action potentials recorded from EPI, ENDO and MID cells, respectively. **b:** Poincaré plots constructed using these sets of action potentials. Individual data (**c**) and average values (**d**) obtained from EPI (n=13/11), ENDO (n=18/14) and MID (n=94/48) myocytes. The stability of SV and APD as a function of time is demonstrated in midmyocardial cells (n=5/4) as shown in panel **e**. Columns and symbols show arithmetic means, bars denote SEM values and asterisks indicate statistically significant ($p<0.05$) differences between groups determined using ANOVA.

Fig. 2 Beat-to-beat variability plotted as a function of action potential duration. **a,b**: Superimposed sets of action potentials recorded from myocytes exposed to current injections, and the corresponding Poincaré plots. Although data were obtained using inward and outward current injections, having amplitudes of -600, -500, -400, -300, -200, -80, -40, 0, +30, +40, +50, +60 and +70 pA, respectively, only the data obtained with -80, -40, 0, +30 and +50 pA are presented in the graph. **c:** SV was plotted against APD for each measurement including the full scale of current amplitudes. Using the non-injected data (zero current) as reference, the current-induced changes in SV (ΔSV) were plotted against the current-induced changes in APD (ΔAPD) in panel **d**. Finally, the ΔSV / ΔAPD ratios were plotted as a function of the corresponding ΔAPD value (**e**). Solid curves were generated by fitting data to monoexponential functions in order to obtain the SV *vs* APD, ΔSV *vs* ΔAPD and ΔSV / ΔAPD *vs* ΔAPD relationships (estimated parameters in Table 1). Results were obtained in 9 myocytes of 8 dogs by analyzing 117 individual data points, i.e. corresponding SV and APD values, each representing a group of 50 consecutive action potentials.

Fig. 3 Effect of the cycle length (CL) of stimulation on beat-to-beat variability. **a,b**: Superimposed sets of action potentials recorded from myocytes paced at various cycle lengths, and the corresponding Poincaré plots. **c,d**: SV and APD, respectively, as plotted as a function of the pacing CL, varied from 0.3 to 5 s. **e**: SV values plotted against the corresponding APD at each CL. The solid curve indicates the SV – APD relationship predicted by the current injection experiments, shown in Fig. **2c**. The experiments were performed in 8 myocytes obtained from 4 dogs. Symbols and bars denote means ± SEM values.

Fig. 4 Dependence of beat-to-beat variability on the intracellular Ca^{2+} concentration ($[Ca^{2+}]_i$). Cells were exposed to the Ca^{2+}-ionophore (1 µM A 23187, n=17/9, **a,b**) or the cell-permeant Ca^{2+}-chelator (5 µM BAPTA-AM, n=31/10, **c**,**d**), then the drug-induced changes in SV and APD were analyzed. Superimposed sets of action potentials (**a,c**) and average results (**b,d**) are presented. Columns and symbols are arithmetic means, bars indicate SEM values, asterisks denote significant differences from control. **e**: Drug-induced changes in SV (ΔSV) plotted against the concomitant change in APD (ΔAPD) compared to the predictions of the previously determined ΔSV-ΔAPD relationship (solid curve).

Fig. 5 Contribution of outward membrane currents to modulation of beat-to-beat variability. Inhibition of the rapid delayed rectifier K^+ current, I_{Kr} (using dofetilide: 10, 30, 100, 300 nM; n = 7/5, 7/5, 30/12, 11/5), the slow delayed rectifier K^+ current, I_{Ks} (using 0.5 µM HMR 1556; n = 11/5), the transient outward K^+ current, I_{to} (using 100 µM chromanol 293B in the presence of HMR 1556; n=17/6), the inward rectifier K^+ current, I_{K1} (using $BaCl_2$: 0.3, 1, 3, 5 µM; n = 6/3, 18/7, 7/3, 27/13), and activation of the ATP-sensitive K^+ current, $I_{K\text{-}ATP}$ (using lemakalim: 0.1, 0.3, 1, 5 µM; n = 6/3, 6/3, 7/3, 6/3), respectively. **a-e:** superimposed sets of action potentials. **f-h:** Drug-induced changes in SV and APD induced by dofetilide (open circles), HMR 1556 (diamond), chromanol 293B (downward triangle), $BaCl_2$ (squares) and lemakalim (upward triangles). The filled circle indicates pooled control. Symbols and bars are means ± SEM values. Solid curves

indicate the SV-APD, ΔSV-ΔAPD and ΔSV/ΔAPD-ΔAPD relationships, obtained from the current injection experiments as shown in Fig. **2c-e**.

Fig. 6 Role of inward currents in the modulation of beat-to-beat variability. Inhibition and activation of the Na^+ current (I_{Na}) and L-type Ca current (I_{Ca}), was performed using tetrodotoxin (TTX: 3 μM, n = 13/5, upward triangle), lidocaine (LID: 50 μM; n = 9/5; downward triangle), veratridine (VER: 10, 30, 100 nM; n = 6/5, 11/5, 19/10; open circles), nisoldipine (NISO: 1 μM; n = 19/13; diamond), and BAY K8644 (20 nM; n = 12/6 and 200 nM; n = 21/9; squares), respectively. **a-e:** Superimposed sets of action potentials. **f-h**: Drug-induced changes in SV and APD. The filled circle represents pooled control, symbols and bars are means ± SEM values. Solid curves indicate the SV-APD, ΔSV-ΔAPD and ΔSV/ΔAPD-ΔAPD relationships, obtained from the current injection experiments as shown in Fig. **2c-e**.

Fig. 7 Effects of ion currents on SV after offsetting their APD-modifying actions. Partial suppression of I_{Kr} (0.1 μM dofetilide, n=7/4, **a**) and I_{K1} (5 μM $BaCl_2$, n=8/4, **b**) as well as the enhanced I_{Na} (0.1 μM veratridine, n=14/5, **c)** and I_{Ca} (0.2 μM BAY K8644, n=10/5, **d**) were compensated by outward currents (OC). Replacement of the suppressed I_{Na} (3 μM tetrodotoxin, n=8/4, **e**) and I_{Ca} (1 μM nisoldipine, n=10/5, **f**) were made by inward current pulses (IC). In these experiments drug-effects on APD were fully offset with current injections having finely adjusted amplitudes so as the pre-drug and post-drug APD values were largely equal. The effects of dofetilide (0.3 μM, n=5/4, **g**) and veratridine (0.1 μM, n=8/4, **h**) on APD were compensated by application of lemakalim, the activator of ATP-sensitive K^+ channels, while in the case of tetrodotoxin (3 μM, n=6/4, **i**) and nisoldipine (1 μM, n=7/4, **j**) properly chosen concentrations of $BaCl_2$ were applied to offset the APD-changes. Columns and bars are means ± SEM, asterisks denote significant differences from control values.

Fig. 8 Effects of isoproterenol on beat-to-beat variability. **a,b**: Superimposed sets of action potentials and Poincaré plots obtained in control and after exposure to 10 nM isoproterenol (ISO). Average ISO-induced changes in APD and SV obtained under

control conditions (n=13/5, **c**) and after 25 min exposure to 5 µM BAPTA-AM (n=7/4, **d**). The corresponding average ΔAPD and ΔSV values are presented in panel **e**.

f-g: Frequency-dependent effects of ISO on APD and SV (n=8/4). The ISO-induced SV-changes (ΔSV) were plotted as a function of the corresponding ΔAPD values and presented in panel **h**, where the bold curve indicates the ΔSV-ΔAPD relationship obtained from current injection experiments. Columns, symbols and bars are means ± SEM, asterisks denote significant ISO-induced changes either in control or in the presence of BAPTA-AM.

Figures

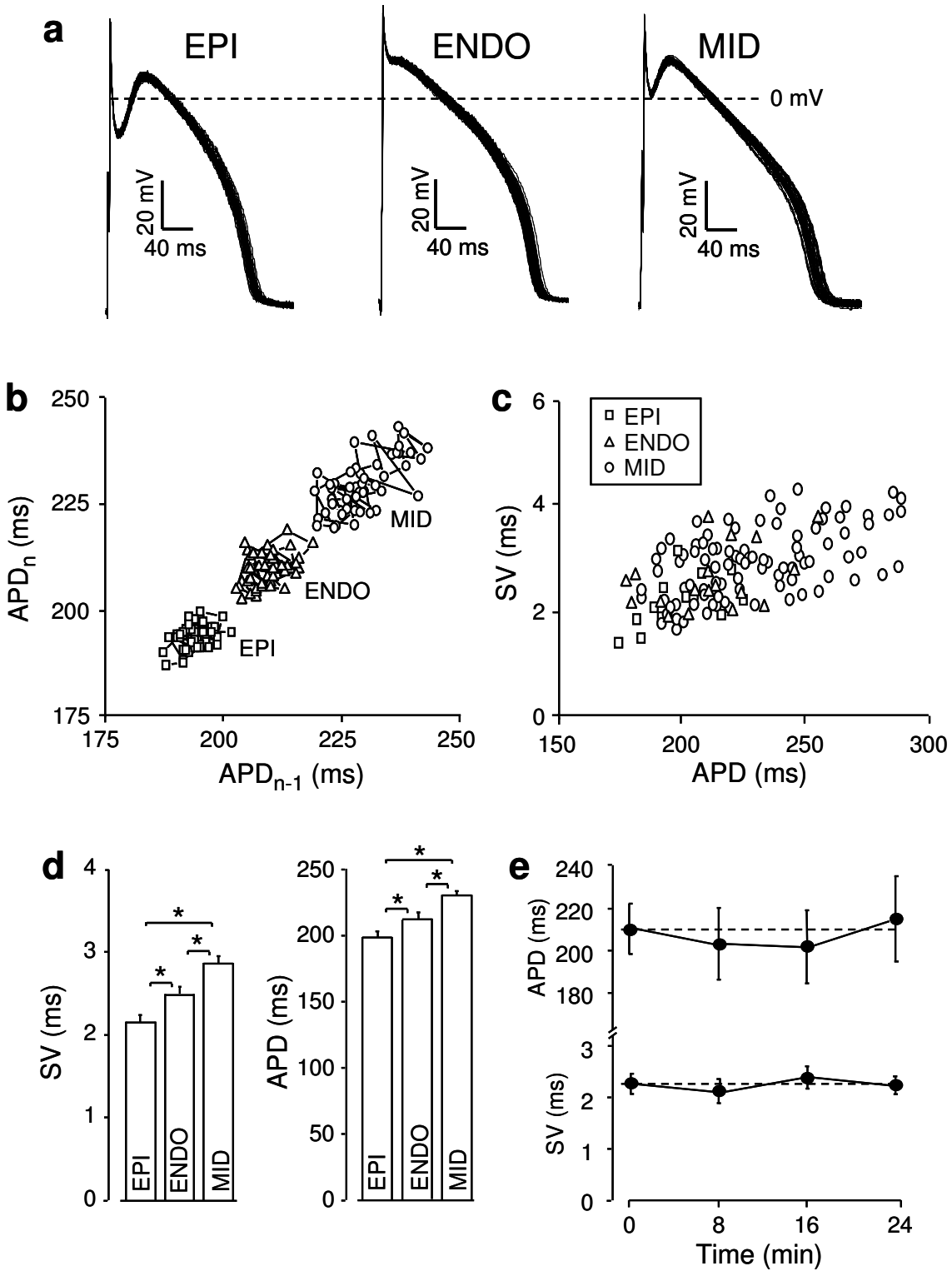

Fig. 1

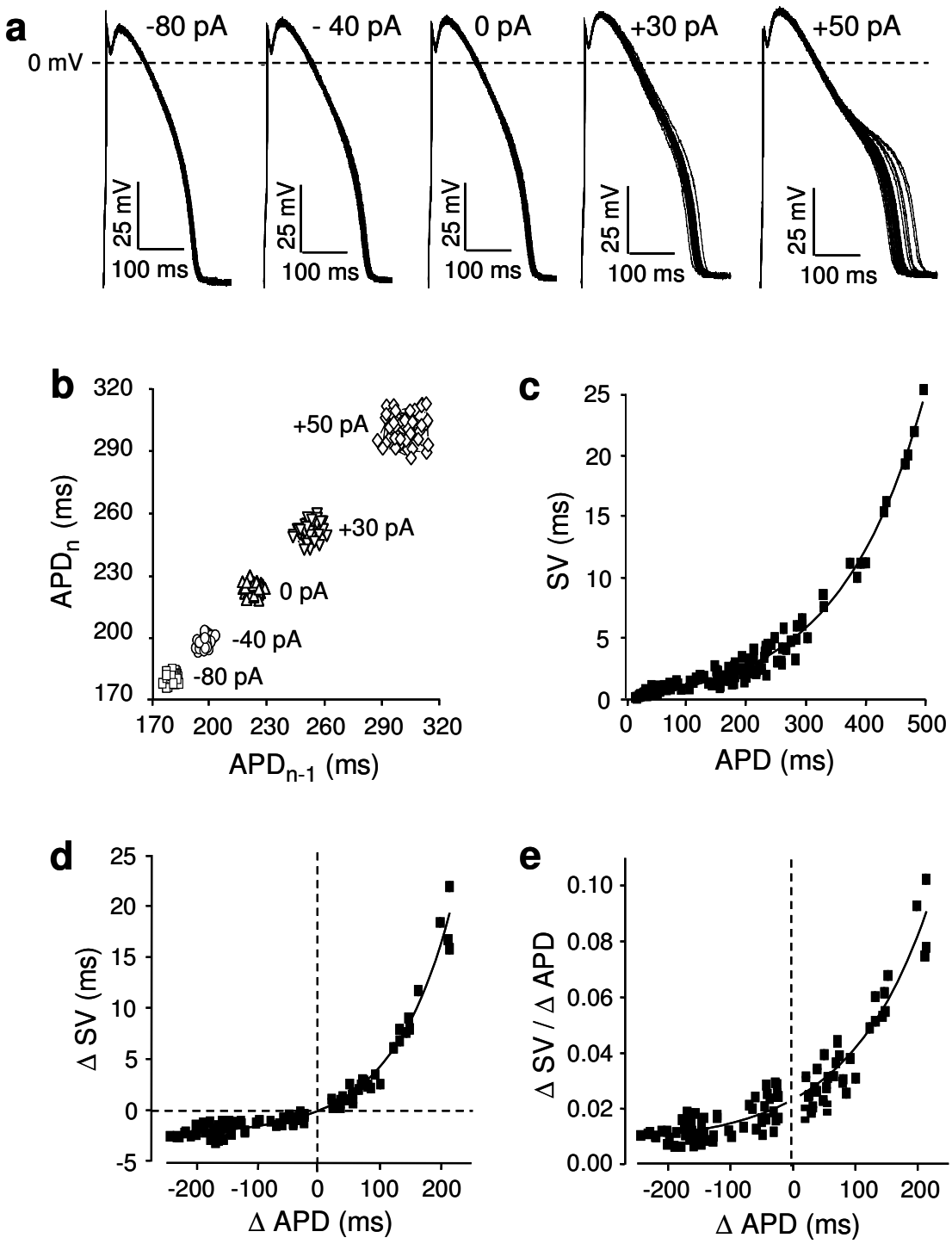
a
-80 pA
- 40 pA
0 pA
+30 pA
+50 pA
0 mV
25 mV
100 ms
b
APDn (ms)
APDn-1 (ms)
+50 pA
+30 pA
0 pA
-40 pA
-80 pA
c
SV (ms)
APD (ms)
d
Δ SV (ms)
Δ APD (ms)
e
Δ SV / Δ APD
Δ APD (ms)

Fig. 2

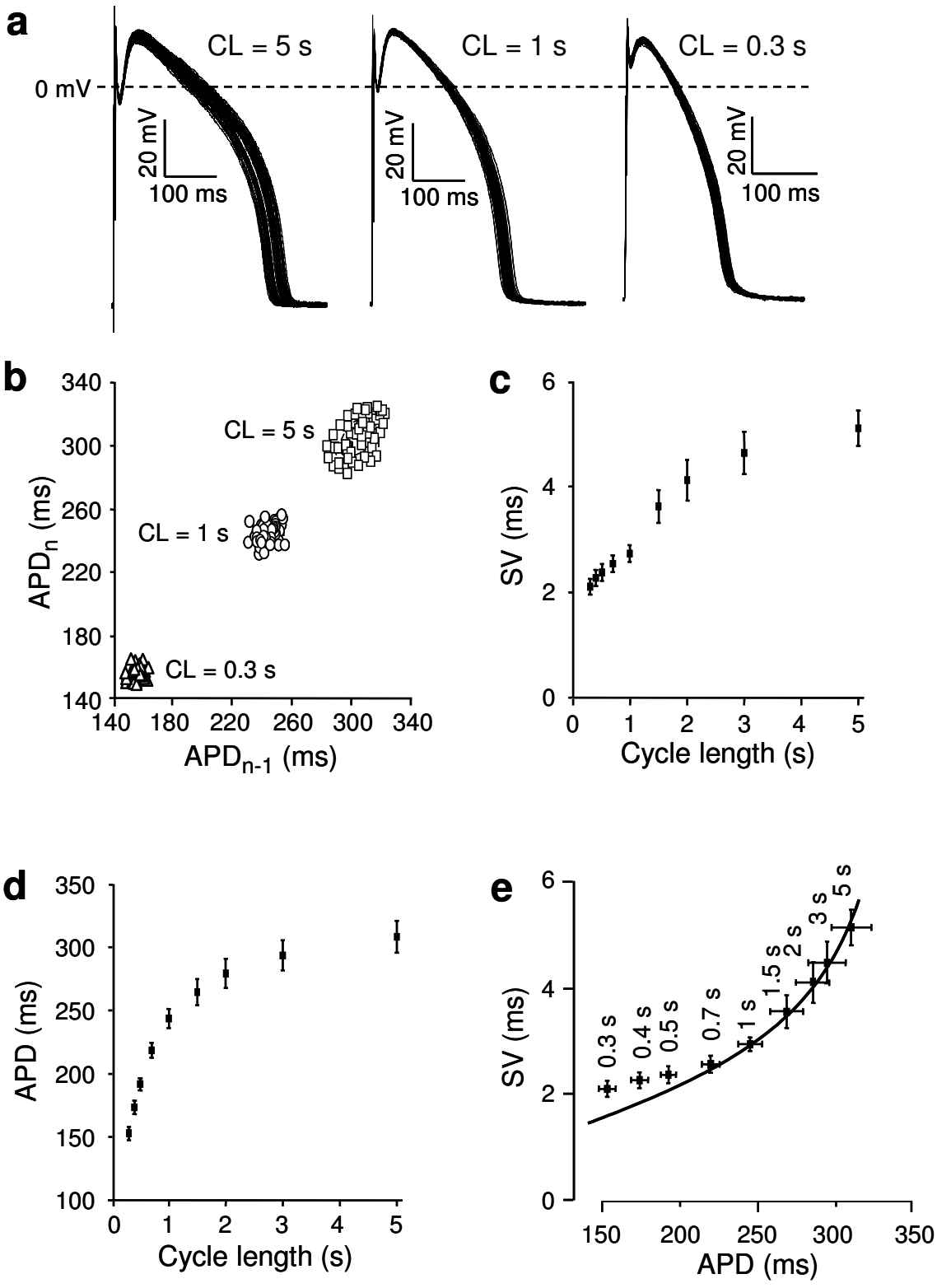
a
CL = 5 s
CL = 1 s
CL = 0.3 s
0 mV
20 mV
100 ms
b
CL = 5 s
CL = 1 s
CL = 0.3 s
APDn (ms)
APDn-1 (ms)
c
SV (ms)
Cycle length (s)
d
APD (ms)
Cycle length (s)
e
SV (ms)
APD (ms)
0.3 s
0.4 s
0.5 s
0.7 s
1 s
1.5 s
2 s
3 s
5 s

Fig. 3

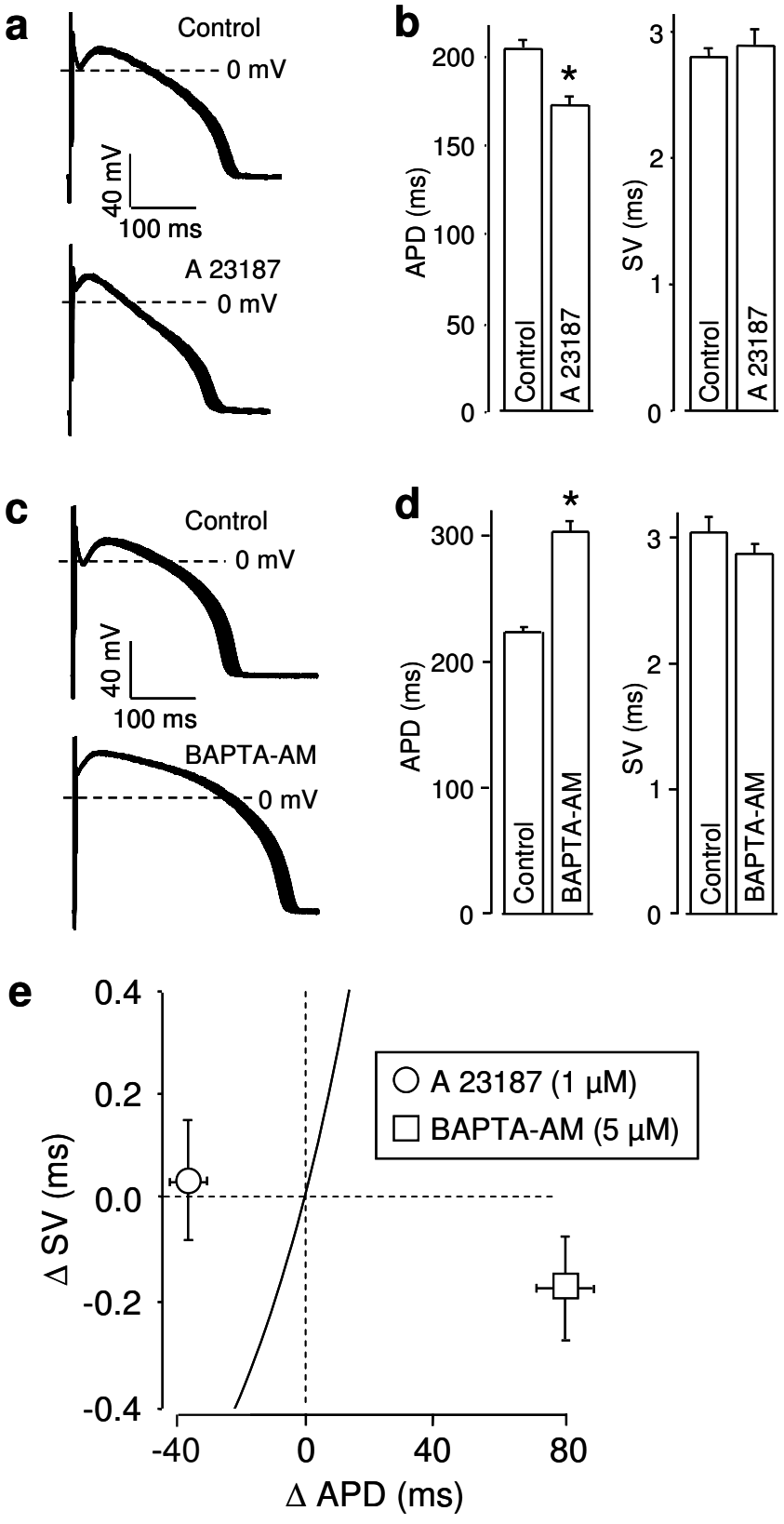
a
Control
0 mV
40 mV
100 ms
A 23187
0 mV
b
APD (ms)
200
150
100
50
0
*
Control
A 23187
SV (ms)
3
2
1
0
Control
A 23187
c
Control
0 mV
40 mV
100 ms
BAPTA-AM
0 mV
d
APD (ms)
300
200
100
0
*
Control
BAPTA-AM
SV (ms)
3
2
1
0
Control
BAPTA-AM
e
Δ SV (ms)
0.4
0.2
0.0
-0.2
-0.4
A 23187 (1 μM)
BAPTA-AM (5 μM)
-40
0
40
80
Δ APD (ms)

Fig. 4

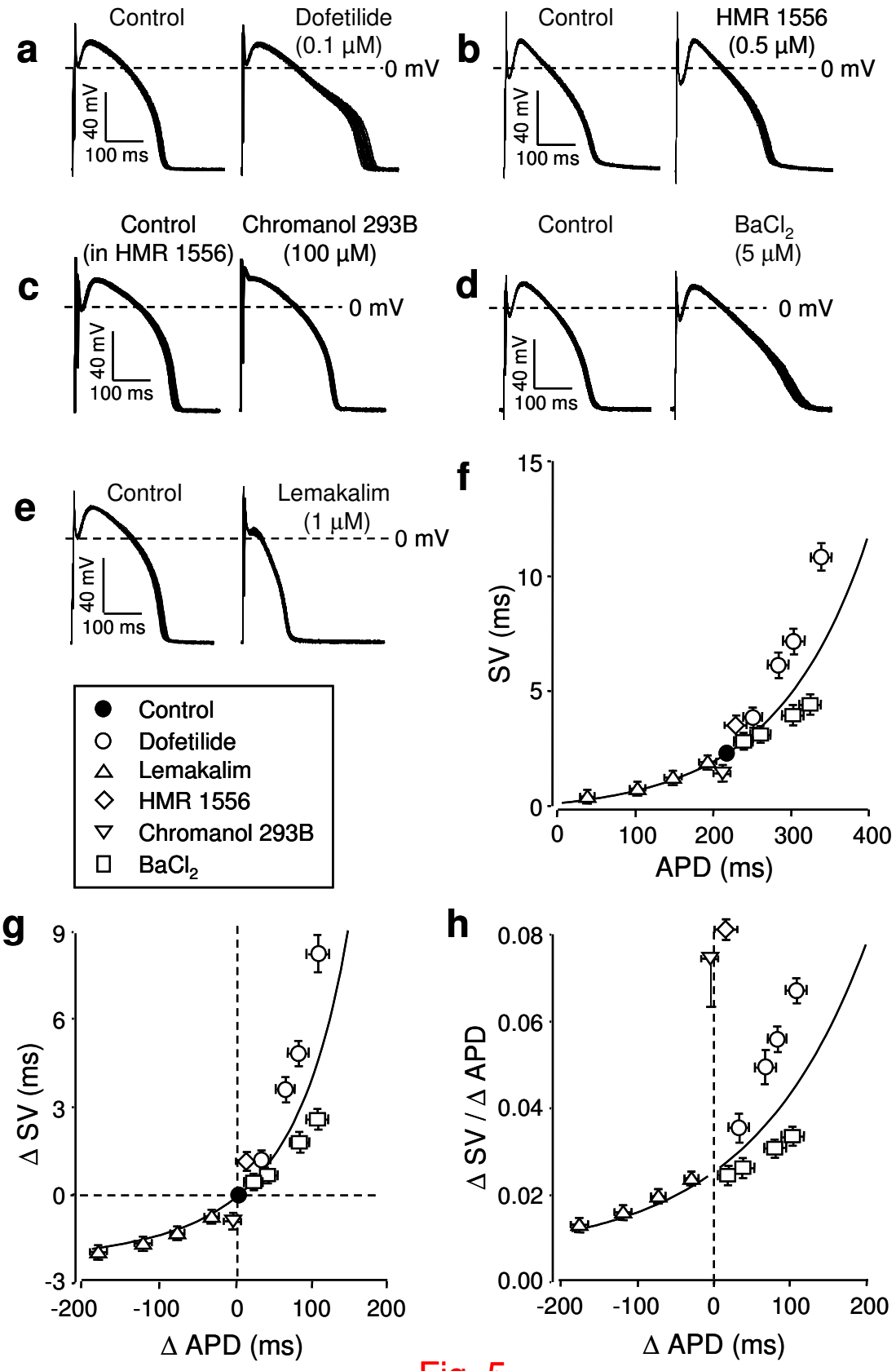
a
Control
Dofetilide
(0.1 µM)
0 mV
40 mV
100 ms
b
Control
HMR 1556
(0.5 µM)
0 mV
40 mV
100 ms
c
Control
(in HMR 1556)
Chromanol 293B
(100 µM)
0 mV
40 mV
100 ms
d
Control
BaCl2
(5 µM)
0 mV
40 mV
100 ms
e
Control
Lemakalim
(1 µM)
0 mV
40 mV
100 ms
Control
Dofetilide
Lemakalim
HMR 1556
Chromanol 293B
BaCl2
f
SV (ms)
APD (ms)
g
Δ SV (ms)
Δ APD (ms)
h
Δ SV / Δ APD
Δ APD (ms)

Fig. 5

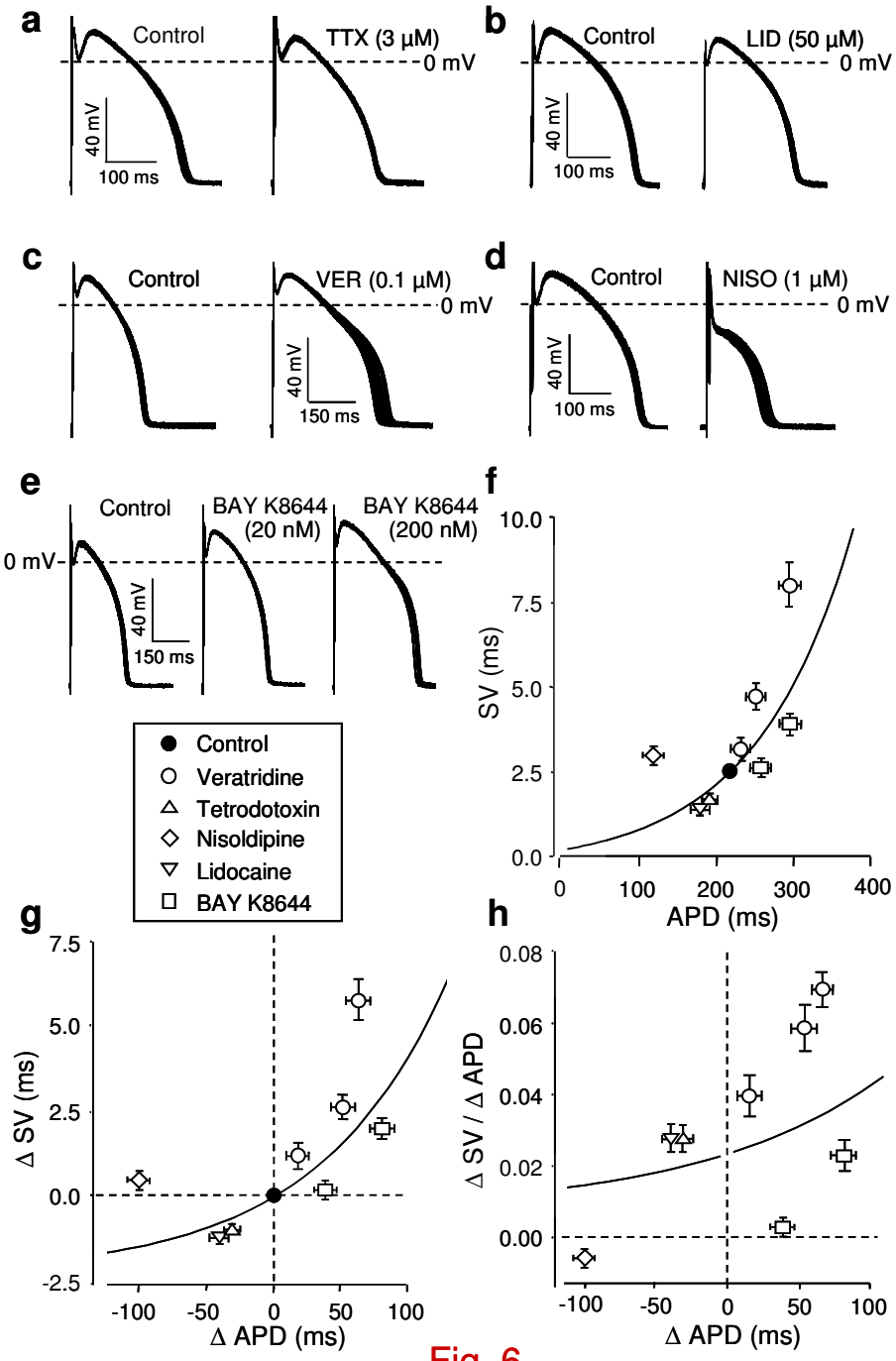
a
Control
TTX (3 µM)
0 mV
40 mV
100 ms
b
Control
LID (50 µM)
0 mV
40 mV
100 ms
c
Control
VER (0.1 µM)
0 mV
40 mV
150 ms
d
Control
NISO (1 µM)
0 mV
40 mV
100 ms
e
Control
BAY K8644 (20 nM)
BAY K8644 (200 nM)
0 mV
40 mV
150 ms
Control
Veratridine
Tetrodotoxin
Nisoldipine
Lidocaine
BAY K8644
f
SV (ms)
APD (ms)
g
Δ SV (ms)
Δ APD (ms)
h
Δ SV / Δ APD
Δ APD (ms)

Fig. 6

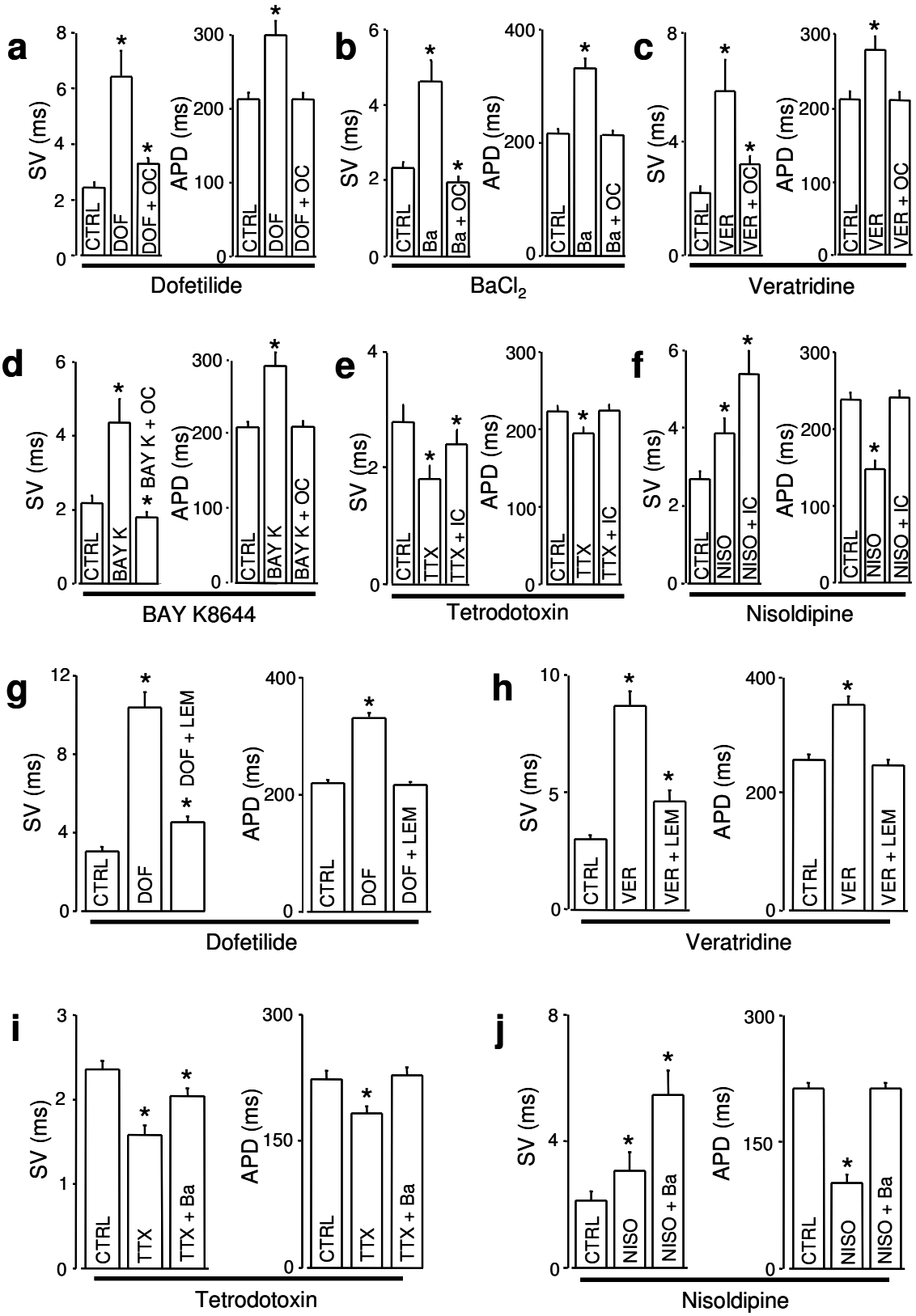
a
SV (ms)
APD (ms)
CTRL
DOF
DOF + OC
Dofetilide
b
Ba
Ba + OC
BaCl2
c
VER
VER + OC
Veratridine
d
BAY K
BAY K + OC
BAY K8644
e
TTX
TTX + IC
Tetrodotoxin
f
NISO
NISO + IC
Nisoldipine
g
DOF + LEM
h
VER + LEM
i
TTX + Ba
j
NISO + Ba

Fig. 7

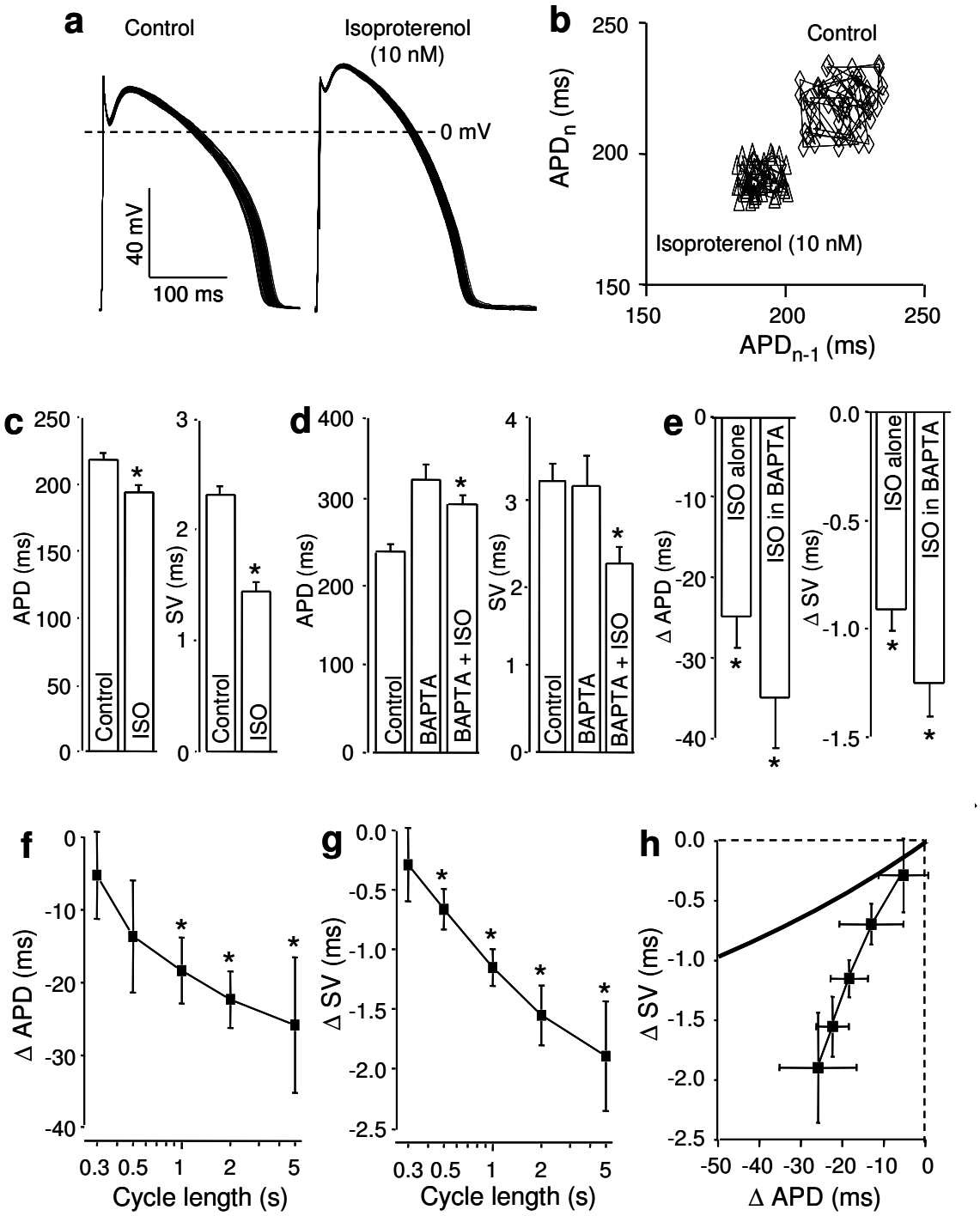
a
Control
Isoproterenol
(10 nM)
0 mV
40 mV
100 ms
b
Control
Isoproterenol (10 nM)
APDn (ms)
APDn-1 (ms)
c
APD (ms)
SV (ms)
Control
ISO
d
APD (ms)
SV (ms)
Control
BAPTA
BAPTA + ISO
e
Δ APD (ms)
Δ SV (ms)
ISO alone
ISO in BAPTA
f
Δ APD (ms)
Cycle length (s)
g
Δ SV (ms)
Cycle length (s)
h
Δ SV (ms)
Δ APD (ms)

Fig. 8